LA-UR-22-31061

Approved for public release; distribution is unlimited.

Title:	Time-Resolved Beam Position Measurements for the Scorpius Multipulse Linear Induction Accelerator
Author(s):	Ekdahl, Carl August Jr. Broste, William B. Johnson, Jeffrey
Intended for:	Report
Issued:	2022-10-19

Time-Resolved Beam Position Measurements for the Scorpius Multipulse Linear Induction Accelerator

Carl Ekdahl, William B. Broste, and Jeffrey Johnson

***Abstract*—Beam position monitors (BPMs) provide time-resolved measurements of the current and centroid position of high-current electron beams in linear induction accelerators (LIAs). One of the types of detectors used in BPMs is the B-dot loop, which generates a signal from the EMF due to the time varying magnetic flux through the loop. If some of the boundaries of the loop are composed of thick metal walls with finite conductivity, the resulting signal must be corrected for the magnetic field diffusion into the metal. The theoretically predicted flux due to diffusion is in remarkable agreement with experimental measurements. Although accurate BPM measurements of beam current require correction of magnetic field diffusion, accurate measurement of beam position requires no correction. In this note, we present a theoretical derivation and the experimental validation of this result.**

***Index Terms*—Linear induction accelerators, electron-beam diagnostics, beam centroid position measurements, beam position monitors, magnetic diffusion**

I. Introduction

FLASH radiography is often used as a diagnostic of explosively-driven experiments. For the largest of these experiments, an intense relativistic electron beam (IREB) is focused onto a target of high-Z metal to create the source spot for point-projection radiography [1, 2]. Linear induction accelerators (LIA) are often used to create the IREB for this diagnostic technique. In the United States, three LIAs are presently used for this purpose [1, 2], and a fourth, called Scorpius, is under development [3, 4].

One of the most important IREB diagnostics for tuning these LIAs to produce radiographic quality beams are the beam position monitors (BPMs) that provide time-resolved measurements of the beam current and the position of the beam centroid. Both of these measurements are critical for tuning and reliable operation of the LIAs.

For our high-current LIAs, BPMs based on detection of the beam magnetic field have proven to be very effective and reliable [5, 6]. The magnetic field detectors for the Scorpius BPMs have a vacuum magnetic-flux detection area bounded on three sides by the metal BPM body. Therefore, diffusion of the magnetic field into the bounding metal contributes to the EMF generated by the time varying field. This effectively increases the detection area in time, resulting in a signal slightly greater than what would be expected based on the geometrical area of the loop. This is most noticeable if the metal is highly resistive, such as stainless steel used for the Scorpius prototype BPM, and field diffusion was evident in initial tests [7, 8]. Therefore, accurate measurement of magnetic flux at the detector location requires correction for diffusion. However, because calculation of the beam centroid position uses the difference between detector signals divided by their sum, beam position measurements do not require correction.

In what follows, we present the theory underlying this important result in Section II, with experimental verification in Section III, followed by a short discussion, and conclusions.

II. Theory

We consider measurements made with a BPM array of azimuthally spaced detectors, as shown in Fig. 1. As illustrated, $[\,r,\theta\,]$ is the position of a filamentary element of the beam current distribution, and $[\,R,\theta_k\,]$ is the position of the k^{th} detector of an array of N magnetic field detectors equally spaced around the beam tube, which has radius R. For Scorpius, initially N=4. These detectors are oriented to be sensitive to B_θ, and their signals are digitally recorded, then analyzed with software.

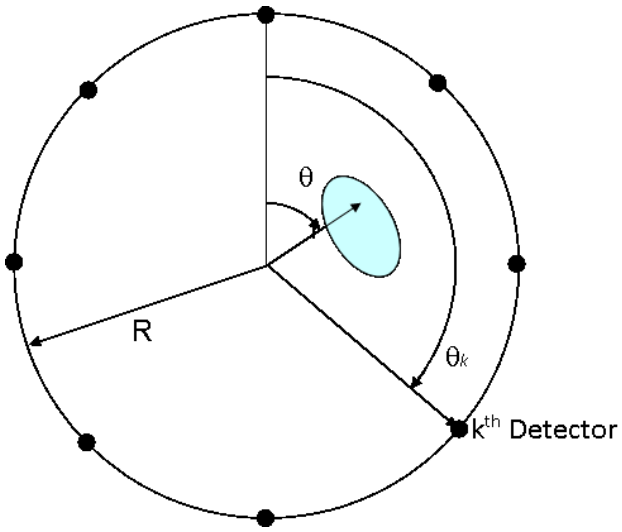

Fig. 1: Conceptual diagram of the location of detectors in a beam position monitor array. In this illustration R is the radius of the detectors, and their azimuthal position is θ_k. A single filament of the beam current distribution (shown in cyan) is located at r,θ.

A. Calculation of Beam Position

The analysis of the signals obtained with this array begins with integration of the raw data (which is proportional to dB_θ / dt), and multiplication by calibration factors as required producing a data record for each detector equal to the azimuthal magnetic field, $B_\theta(R,\theta_k)$. To resolve the m^{th} azimuthal harmonic of the field these records are multiplied by either $\sin m\theta_k$ or $\cos m\theta_k$ and summed to yield:

$$\sigma_m^s = \sum_{k=1}^{N} B_\theta(R,\theta_k)\sin m\theta_k \quad , \qquad (1)$$

and

$$\sigma_m^c = \sum_{k=1}^{N} B_\theta(R,\theta_k)\cos m\theta_k \quad . \qquad (2)$$

As shown in Ref. 1, these sums are related to the position of a single current element of the distribution located at [r,θ] by

$$\sigma_m^s = N\frac{\mu_0 i}{2\pi R}\left(1+\varepsilon_{m,N}^s\right)\rho^m \sin m\theta \quad , \qquad (3)$$

and

$$\sigma_m^c = N\frac{\mu_0 i}{2\pi R}\left(1+\varepsilon_{m,N}^c\right)\rho^m \cos m\theta \quad . \qquad (4)$$

Here i is the filamentary current, $\rho^m = (r/R)^m$, and the $\varepsilon_{m,N}^{s,c}$ are small aliasing errors resulting from the discrete nature of the detector array, which are insignificant for [9]. $\rho^m << 1$. Eq. (3) and (4) can be used as Green's functions to find the relation between the harmonic array sums (Eq. (1) and Eq. (2) moments of the current distribution by integrating over the distribution, and recalling the defining equation for moment analysis;

$$\langle f(x,y)\rangle = \frac{\iint f(x,y)\,j(x,y)\,dx\,dy}{\iint j(x,y)\,dx\,dy} = \frac{1}{I}\iint f(x,y)\,j(x,y)\,dx\,dy \quad . \qquad (5)$$

The first (m =1) harmonic is required for determination of beam position, and performing that integration one has

$$\Sigma_1^s = N\frac{\mu_0 I}{2\pi R}\frac{\langle x\rangle}{R} \quad , \qquad (6)$$

$$\Sigma_1^c = N\frac{\mu_0 I}{2\pi R}\frac{\langle y\rangle}{R} \quad , \qquad (7)$$

where

$$\Sigma_m^{c,s} \equiv \langle \sigma_m^{c,s}\rangle \qquad (8)$$

.

Equations (6) and (7) are supplemented by the direct, unweighted sum of all N detectors;

$$\Sigma_0 = N\frac{\mu_0 I}{2\pi R} \quad , \qquad (9)$$

which is used as a normalization factor to finally obtain:

$$\langle x\rangle = R\frac{\Sigma_1^s}{\Sigma_0} \quad , \qquad (10)$$

$$\langle y\rangle = R\frac{\Sigma_1^c}{\Sigma_0} \quad , \qquad (11)$$

These two equations give the position of the center of the beam current. For a four-detector array, these simplify to

$$\langle x\rangle = R\frac{B_{\theta,1}-B_{\theta,3}}{B_{\theta,1}+B_{\theta,2}+B_{\theta,3}+B_{\theta,4}} \equiv R\frac{\Delta_x}{\Sigma_0} \qquad (12)$$

$$\langle y\rangle = R\frac{B_{\theta,2}-B_{\theta,4}}{B_{\theta,1}+B_{\theta,2}+B_{\theta,3}+B_{\theta,4}} \equiv R\frac{\Delta_y}{\Sigma_0} \qquad (13)$$

B. Magnetic-Field Diffusion

The field detectors of new BPMs under development for Scorpius are known to exhibit effects due to diffusion of the magnetic field into the bounding conductor, because the metal is highly resistive stainless steel, a common construction material for high vacuum accelerator components. The diffusion of field into the bounding metal effectively increases the detection area in time, resulting in a signal slightly greater than what would be expected based on the geometrical area of the loop.

$$\mathcal{E} = -\frac{\partial\Phi}{\partial t} = -A_0\frac{\partial B_\theta}{\partial t} - \frac{\partial\Phi_D}{\partial t} \qquad (14)$$

for the radial dimension of the cavity small compared to the radius of the outer wall. Here, the first right-hand term is the emf in the absence of diffusion, where A_0 is the area bounded by the vacuum cavity walls and the coaxial sensing pin, B_θ is the average azimuthal magnetic field in the cavity.

The total flux contributing to the signal, Φ , includes both that linking the area of the vacuum cavity and the flux diffusing into the metal, Φ_D . Integrating, either by hardware, software, or a combination of both, gives

$$B_\theta = (\Phi - \Phi_D)/A_0 \qquad (15)$$

where the slight difference from equality is corrected through careful calibration. Here, from Eq. (14), the total flux is the integral of the detected emf signal

$$\Phi(t) = \int_0^t \mathscr{E}(t')dt' \tag{16}$$

which must be corrected according to Eq. (15) to give the actual magnetic field. Methods for correcting the signals based on calibration experiments are fully described in theory and practice in ref. [10, 11, 12].

Eq. (15) can be rearranged and reformulated as

$$B_\theta = B_m\left(1-\varepsilon_D\right) \tag{17}$$

where B_m is the uncorrected measurement, $B_m(t) = \Phi(t)/A_0$ and $\varepsilon_D(t)$ is the error due to diffusion. Inserting into Eq. (12) and one has

$$\langle x\rangle = R\frac{\Delta_{x,m}\left(1-\varepsilon_D\right)}{\Sigma_{0,m}\left(1-\varepsilon_D\right)} = R\frac{\Delta_{x,m}}{\Sigma_{0,m}} \tag{18}$$

with similar results for $\langle y\rangle$, showing that no correction for diffusion is needed for calculating the beam centroid position. This theoretical result was experimentally validated with a prototype Scorpius BPM.

III. EXPERIMENTAL VALIDATION

The theoretical results of Section II result were corroborated with data taken in two experimental configurations.

First, we used data obtained during calibration of the Scorpius prototype detector on the air-insulated high-voltage coaxial transmission line that was used to calibrate DARHT-II BPMs [6, 7]. The inner conductor of this test line can be accurately moved to positions offset from the center in both horizontal (x) and vertical (y) directions to effect calibration of position measurements [13]. For beam centroid position measurements, the calibrated DARHT-II BPM data is analyzed using a computer code (named D2_BDOT) that embodies the equations in the preceding Section II [14].

The second configuration involved the fielding of the Scorpius BPM prototype on the DARHT-II beam line ahead of a standard DARHT-II BPM (number 29) in the post-kicker transport region, just before the final focus magnet. Comparison of the current and position data from that experiment with the full energy four-pulse DARHT-II beam will be made in a report in preparation. For purposes of this note, results from that experiment will be limited to a representative sample of position data as calculated without diffusion correction.

It is appropriate at this juncture to present a brief discussion of analysis methods. The equations presented in Section II have been realized in a multitude of ways over the history of the use of magnetic beam sensing loops. In the development and commissioning of DARHT-II, the use of those equations was put into use with coding in the IDL software language [15], and very carefully vetted against alternate means of computation to ensure its accuracy. When used for monitoring of the position and current on DARHT-II, the analysis was vested in the D2_BDOT code that has been maintained under careful configuration management. Further, once the file structure and data storage formats for DARHT-II had been solidified, a set of simulation files was created based on analytically defined beam parameters. This simulation set was then used to ensure that the analysis software was correctly computing beam properties as the D2_BDOT code evolved over the years. For a project as complex and critical as Scorpius, a similar verification process is highly recommended.

For the data presented in this note, the position analysis using both the diffusion corrected data and the data without diffusion correction was performed using a carefully modified version of the fundamental D2_BDOT coding. The modified code was verified against the most recent standard configuration, for the analysis without diffusion correction. The diffusion correction process had been checked against alternate computational methods as reported previously [7, 8, 9]. All of the data presented in the following sections was taken with resistors mounted in-line at the output of the Scorpius prototype, prior to connection to the transmission line leading to the recording digitizers. While this hardware implementation results in recorded signals one-half of what could be obtained without the in-line impedance matching resistors, it is the best way to preserve signal bandwidth and prevent undesirable reflections when signal-recording time exceeds the two-way transit time between detector and recorder.

A. Test-line Validation

The standard process of BPM calibration with the test line involves measurements of detector output for twenty-nine pulses from the current source. Thirteen are on axis, and the remaining sixteen are divided equally between X and Y displacements for the current center from +/-1.26 to 6.32 mm. The pulses were slightly slower than the design goal of 10ns 10-90% rise for Scorpius, but comparable in length, ~100ns. As a reminder of the need for diffusion correction in computing current, Fig. 2 compares the uncorrected, diffusion corrected, and reference pulse (from a calibrated resistor string at the end of the coaxial line) shapes for a typical test line recording.

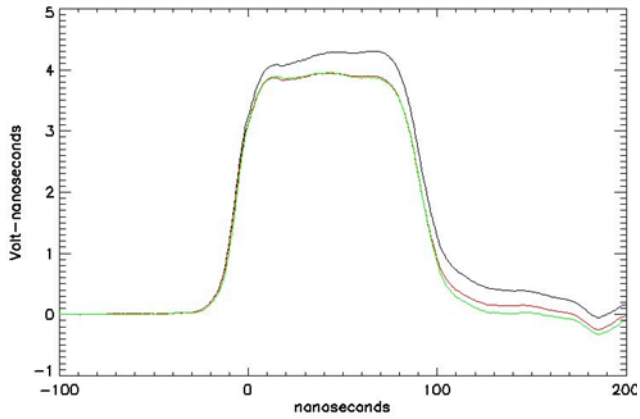

Fig. 2: Comparison of b-dot output and its correction. Black Curve: Raw data. Red Curve: Data after correction. Green Curve: Reference pulse normalized to corrected data.

Fig. 3 and Fig. 4 present computations of the X and Y positions, with and without diffusion correction, with the center conductor positioned to give current center at X or Y =3.8 mm Conductor positioning probable error is 100 microns, so the diffusion/no-diffusion difference is well within the errors inherent in the calibration.

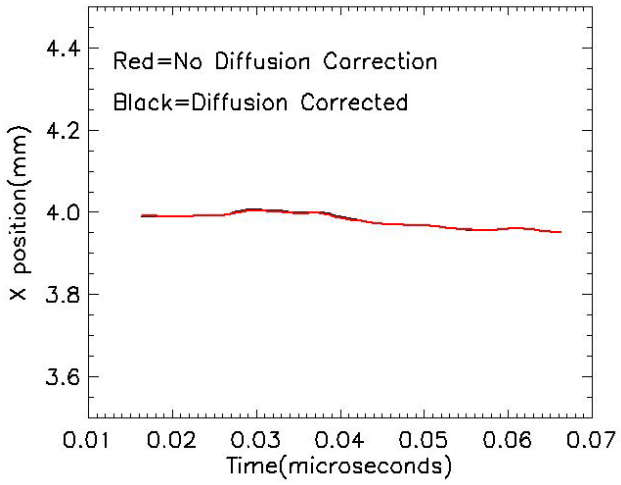

Fig. 3: Measured test-line inner conductor horizontal position with correction for diffusion (black curve) and without diffusion correction (red curve), showing apparent drift due to variation of diffusion among detectors. (Note that this plot magnifies this systematic error by zooming in on measured position.)

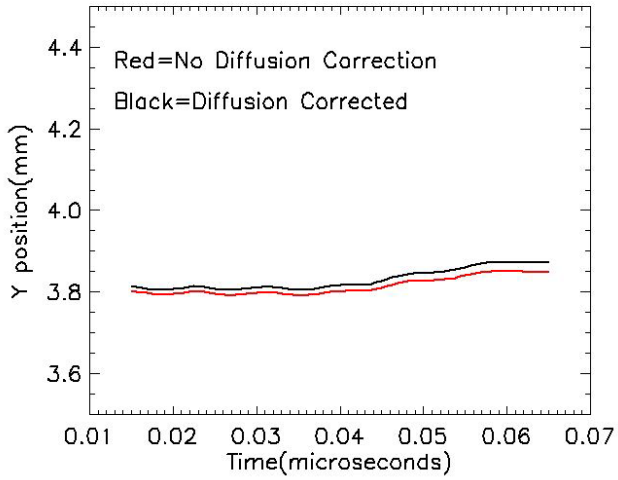

Fig. 4: Measured test-line inner conductor vertical position with correction for diffusion (black curve) and without diffusion correction (red curve), showing apparent drift due to variation of diffusion among detectors. (Note that this plot magnifies this systematic error by zooming in on measured position.)

Obviously, any measurement of the position of the test-line inner conductor should be constant in time. Time varying results provide an estimate of the uncertainty of the proposition that field diffusion is the same for all four B-dot detectors. For example, the apparent drift of the measured inner conductor position shown in Fig. 3 and Fig. 4 is a systematic error likely due to variation of diffusion among the four B-dot detectors. Therefore, the ~0.5% rms deviation from the mean horizontal position (3.98 mm), and the ~0.6% rms deviation from the mean vertical position (3.82 mm) might be a good estimate of the practical uncertainty of position measurements with the Scorpius BPMs.

The difference between the two analysis methods as illustrated in Figure 4 is .016 out of 3.8 (0 .4%.) The diffusion correction involves using finite approximations to pulse shape, so small differences in diffusion/no-diffusion results can be expected for different data sets produced by different source pulses (e.g., the X position and Y position were measured with two different configurations of the test-line inner conductor on two different pulses).

In summary, the measurements on the testline validate the theoretical prediction that beam position measurements need not be corrected for diffusion, to within an uncertainty of less than 1%.

B. Electron Beam Validation

The Scorpius prototype was installed on the DARHT-II beam line as a companion experiment to ongoing tests of target configurations. In that circumstance, the Scorpius tests of necessity obtained data on the multi-pulse train as dictated by the primary experiment. Further, because the recording system had been configured prior to the discovery of the baseline zero variability problem with the available digitizers, only the first pulse in the four-pulse sequence has been

accurately processed for much of the data. Full data recovery is a work in progress. Nevertheless, the data from the first pulse provides a useful platform for evaluation of the need for diffusion correction. As for the test line data, the first plot for this set, Fig. 5, compares the current calculation with and without diffusion correction.

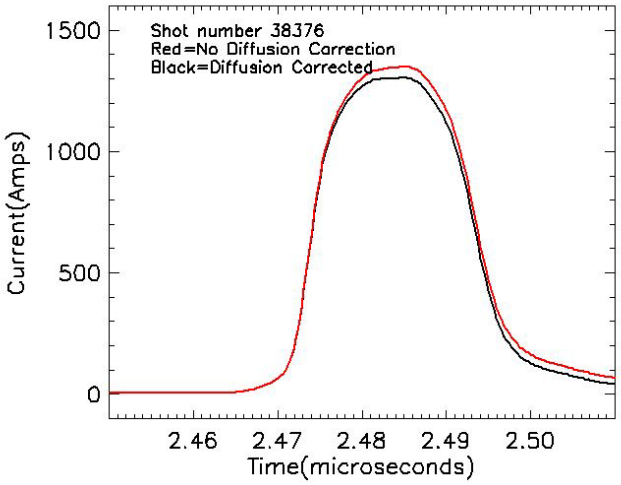

Fig. 5: DARHT-II Current Pulse with and without diffusion correction.

Because the pulse is quite short, the peak level of the diffusion error is fractionally lower than for the test line data. For this data, there is no "known" position, although the results from the Scorpius prototype are equivalent to the results from the nearby standard DARHT-II BPM29 within the measurement uncertainty of the location of the two detector spools. Fig. 6 and Fig. 7compare the beam position as calculated with and without diffusion correction for shot 38376 on September 23, 2021.

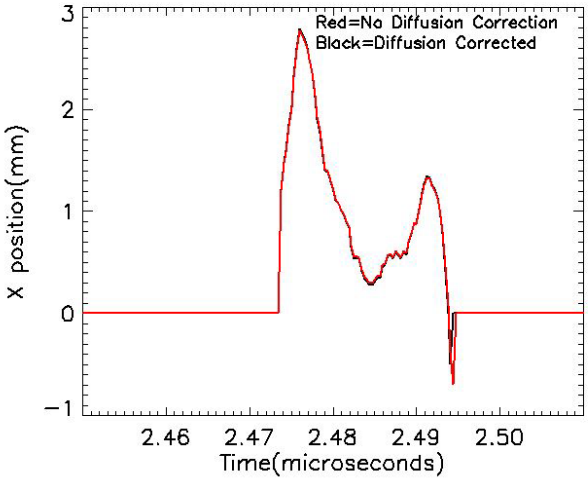

Fig. 6: X Position of the DARHT-II beam calculated with and without diffusion correction.

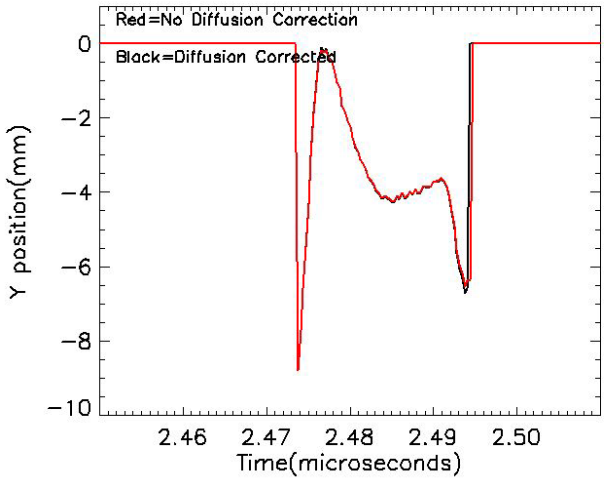

Fig. 7: Y Position of the DARHT-II beam calculated with and without diffusion correction.

Both of the position plots have been restricted to portions of the record where beam current was more than 500 Amps to avoid confusing the comparison with positions when the denominator in equations (12) and (13) is small.

A further test of the Scorpius BPMs was a comparison with the DARHT-II BPMs. The beam position is not expected to be the same at these two locations. If the beam is incident at an angle, there would be a constant offset of position between the two BPMs. Moreover, beam corkscrew motion would cause a time-varying difference between the two BPMs. Nevertheless, the comparison is a useful check of the accuracy of Scorpius BPM position measurements in the operational environment. The results are illustrated in Fig. 8 and Fig. 9. Although there is some evidence of beam corkscrew motion Fig. 8, the lack of a constant offset between the position curves is an indication that the beam trajectory was parallel to the axis for this pulse. From these plots, it is evident that the uncorrected position measurement with the Scorpius BPMs was in reasonable agreement with the position measured with the DARHT BPM for the first pulse of this burst.

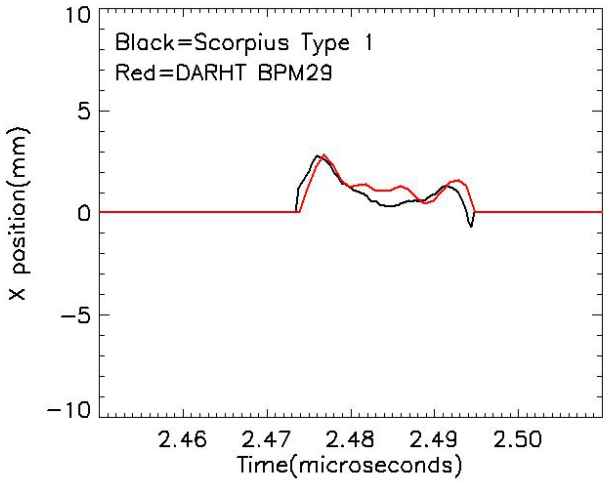

Fig. 8: Comparison of uncorrected Scorpius BPM measurement of beam centroid horizontal position (black curve) with horizontal position measured with DARHT-II BPM (red curve).

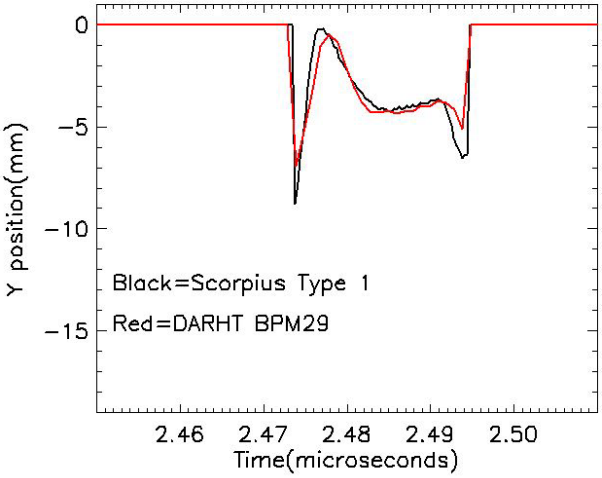

Fig. 9: Comparison of uncorrected Scorpius BPM measurement of beam centroid vertical position (black curve) with vertical position measured with DARHT-II BPM (red curve).

IV. DISCUSSION

Although accurate measurement of beam current with the Scorpius BPM requires correction of magnetic field diffusion into the stainless steel, the data as presented make it clear that accurate measurement of beam position requires no correction.

The derivation of this result assumes that the error due to diffusion is the same for all detectors. If not, there is a small uncertainty in using uncorrected data for position measurements. If the standard deviation of the diffusion error among the four detectors is measured to be σ% during calibration, then propagation of errors suggests that the uncertainty in position due to the variation of diffusion time among detectors would be about 2.4σ%. Because the diffusion correction ε_D is small, it is difficult to determine its value to much better than a 5% relative uncertainty. But, by the same circumstance, a 5% uncertainty in a 10% effect means that σ in the preceding argument is .005 of the total signal values, leading to a 1.2% uncertainty in position. For reasonable tuning operations, where positions should be within 5mm of center, neglecting the worst possible diffusion variability would lead to position errors of <60 microns. With that level of uncertainty prior to the final focus, on-target position errors will be very small from using the uncorrected position data.

V. CONCLUSION

We have shown that calculation of the beam centroid position from BPM data needs no correction for magnetic field diffusion effects in the B-dot detectors. The underlying theory was validated experimentally on a calibration transmission line, as well as by comparing DARHT-II multipulse beam measurements made with a Scorpius BPM with those made with a standard DARHT-II BPM. Based on these experiments, the uncertainty in measured beam centroid position due to not correcting for diffusion was determined to be less than 1% for the Scorpius prototype BPM.

ACKNOWLEDGMENT

The authors wish to thank their colleagues at Los Alamos and elsewhere for years of stimulating discussions about relativistic electron beam physics, linear induction accelerators, and other topics.

This work was supported by the U.S. Department of Energy through the Los Alamos National Laboratory. Los Alamos National Laboratory is operated by Triad National Security, LLC, for the National Nuclear Security Administration of U.S. Department of Energy (Contract No. 89233218CNA000001).

REFERENCES

[1] C. Ekdahl, "Modern electron accelerators for radiography," *IEEE Trans. Plasma Sci.,* vol. 30, no. 1, pp. 254-261, 2002.

[2] K. Peach and C. Ekdahl, "Particle radiography," *Rev. Acc. Sci. Tech.,* vol. 6, pp. 117 - 142, 2013.

[3] M. T. Crawford and J. Barraza, "Scorpius: The development of a new multi-pulse radiographic system," in *Proc. 21st IEEE Int. Conf. Pulsed Power*, Brighton, UK, 2017.

[4] M. Crawford, J. Barraza and C. Ekdahl, "Scorpius update: Progress toward a new multi-pulse radiographic system," in *IEEE Pulsed Power Conference*, Denver, CO, USA, 2021.

[5] C. Ekdahl, E. O. Abeyta, H. Bender, W. Broste, C. Carlson, L. Caudill, K. C. D. Chan, Y.-J. Chen, D. Dalmas, G. Durtschi, S. Eversole, S. Eylon, W. Fawley, D. Frayer, R. Gallegos, J. Harrison, E. Henestroza, M. Holzscheiter, T. Houck, T. Hughes, S. Humphries, D. Johnson, J. Johnson, K. Jones, E. Jacquez, B. T. McCuistian, A. Meidinger, N. Montoya, C. Mostrom, K. Moy, K. Nielsen, D. Oro, L. Rodriguez, P. Rodriguez, M. Sanchez, M. Schauer, D. Simmons, H. V. Smith, J.

Studebaker, R. Sturgess, G. Sullivan, C. Swinney, R. Temple, C. Y. Tom and S. S. Yu, "Initial electron-beam results from the DARHT-II linear induction accelerator," *IEEE Trans. Plasma Sci.,* vol. 33, no. 2, pp. 892 - 900, 2005.

[6] J. Johnson, C. Ekdahl and W. Broste, "DARHT axis-II beam position monitors," in *AIP Conference Proceedings, vol. 732(1)*, 2004.

[7] J. Johnson and K. Bishofberger, "Initial testing of Scorpius beam position monitorsthe," Los Alamos National Laboratory Report LA-UR-21-28704, September, 2021.

[8] C. Ekdahl, W. B. Broste and J. Johnson, "Magnetic-Field Diffusion Effects in Beam Position Monitors I: Theory," Los Alamos National Laboratory report LA-UR-22-, 2022.

[9] C. Ekdahl, "Aliasing errrors in measurements of beam position and ellipticity," *Rev. Sci. Instrum.,* vol. 76, p. 095108, 2005.

[10] C. Ekdahl, W. B. Broste and J. Johnson, "Magnetic-Field Diffusion Effects in Beam Position Monitors I: Theory," Los Alamos National Laboratory Report LA-UR-22-26981, 2022.

[11] W. B. Broste, C. A. Ekdahl and J. B. Johnson, "Magnetic-Field Diffusion Effects in Beam Position Monitors II:Application to Calibration Single-Pulse Data," Los Alamos National Laboratory Report LA-UR-27535, 2022.

[12] C. Ekdahl and W. B. Broste, "Correcting magnetic-field diffusioneffects in beam position monitors," Los Alamos National Laboritory Report LA-UR-22-27765, 2022.

[13] C. Ekdahl, S. Eversole, H. Olivas, P. Rodriguez, B. Broste, J. Johnson and E. Petersen, "DARHT-II beam position monitor B-dot owner's manual," Los Alamos National Laboratory Report LA-UR-22-29698, 2002.

[14] C. Ekdahl, "Using the D2_BDOT analysis code," Los Alamos National Laboratory Report LA-UR-22-, 2007.

[15] "IDL Software," L3Harris, [Online]. Available: https://www.l3harrisgeospatial.com/Software-Technology/IDL. [Accessed 2022].